

LOCI OF 3-PERIODICS IN AN ELLIPTIC BILLIARD: WHY SO MANY ELLIPSES?

RONALDO GARCIA, JAIR KOILLER, AND DAN REZNIK

ABSTRACT. A triangle center such as the incenter, barycenter, etc., is specified by a function thrice- and cyclically applied on sidelengths and/or angles. Consider the 1d family of 3-periodics in the elliptic billiard, and the loci of its triangle centers. Some will sweep ellipses, and others higher-degree algebraic curves. We propose two rigorous methods to prove if the locus of a given center is an ellipse: one based on computer algebra, and another based on an algebro-geometric method. We also prove that if the triangle center function is rational on sidelengths, the locus is algebraic.

Keywords: Poncelet, porism, locus, resultants, algebraic

MSC2010 37-40 and 51N20 and 51M04 and 51-04

1. INTRODUCTION

Classic notable points of a triangle include the incenter, barycenter, orthocenter, and circumcenter, see Appendix A.1 for a refresher. While these are traditionally obtained via geometric constructions, Kimberling has generalized this to *triangle centers* [15], specified by a *triangle function*, thrice-applied (in cyclical fashion) to the sidelengths and/or angles of a triangle, thus forming a triple of *trilinear coordinates*. These are reviewed in Appendix A.2.

Thousands of such centers are catalogued in Kimberling's Encyclopedia of Triangle Centers (ETC) [16]. Centers are labeled X_i , e.g., the incenter is X_1 , the barycenter X_2 , etc. For each center the corresponding triangle function is provided. A quick perusal reveals these to be either rational, irrational, or more rarely, transcendental, on the sidelengths and/or angles of a triangle.

Consider the 1d family of 3-periodic orbits in the elliptic billiard (EB), Figure 1. The vertices are bisected by ellipse normals and the sides are tangent to a virtual confocal caustic; see Appendix B for a review. We have been drawn to this family because unexpectedly, the locus of the incenter is an ellipse and that of the Mittenpunkt¹ X_9 is the billiard center [23]. Additionally, many other curious invariants have been detected and/or proved [1, 2, 24].

¹This point was discovered by Nagel in 1836 as the point of concurrence of lines from the excenters through side midpoints [33], see Figure 10 (right).

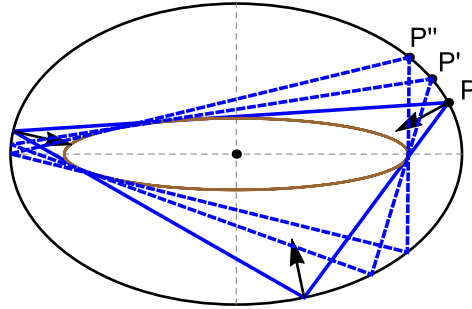


FIGURE 1. Three 3-periodic orbits (one solid with vertex P and two dashed with vertices P' , P''). The vertices are bisected by ellipse normals and the sides are dynamically tangent to a virtual confocal caustic (brown). Remarkably, the family conserves perimeter [31]. [app](#)

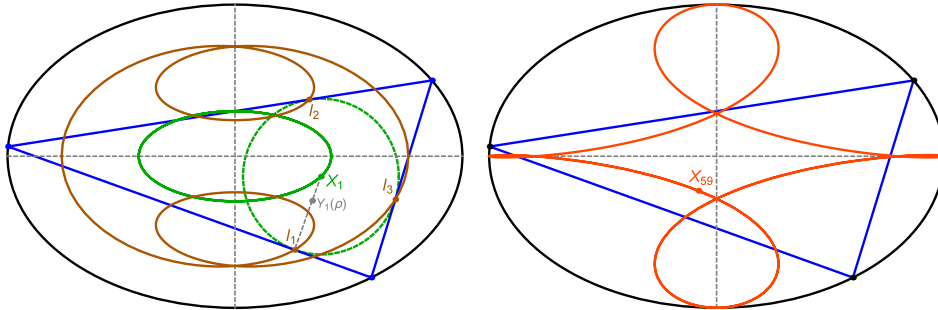


FIGURE 2. **Left:** A sample 3-periodic orbit (blue), the elliptic locus of the Incenter X_1 (green) and of that of the Intouchpoints I_1, I_2, I_3 (brown), the points of contact of the Incircle (dashed green) with the orbit sides. These produce a curve with two internal lobes whose degree is at least 6. $Y_1(\rho)$ is a convex combination of X_1 and I_1 referred to in Section 2.5. [app](#), [Video 1](#), [Video 2](#). **Right:** The locus of X_{59} is a curve with four self-intersections. A vertical line epsilon away from the origin intersects the locus at 6 points. [app](#)

In general, triangle centers sweep such curves as ellipses, quartics, sextics, etc., with or without self-intersections, etc.; see Figure 2. The central question here is: given a triangle center, is it possible to predict its locus curve type over billiard 3-periodics based on the triangle function?

Main Results. We present a hybrid numerical-CAS (Computer Algebra System) method to rigorously verify if the locus of given triangle center is an ellipse or not. We apply it to the first 100 centers listed in [16], finding that 29 are elliptic. We have derived explicit expressions for their axes [9] (Theorem 1).

We consider the curious case of the Symmedian Point X_6 , whose locus closely approximates an ellipse but using CAS-based manipulation, we show it is actually a quartic (Theorem 2), which we derive explicitly. Interestingly, its triangle function is rational on the sidelengths and is one of the simplest on the whole of [16]; see Table 6 in Appendix A.1.

Using algebro-geometric techniques, we prove (Theorem 3) that when the trilinear coordinates (defined in Appendix A.2) of a triangle center are rational on the orbit's sidelengths, the locus is an algebraic curve (elliptic or otherwise). We also describe an algorithm based on the method of resultants which computes the zero set of a polynomial in two variables corresponding to the locus. After extensive experimentation, we haven't yet found a non-rational triangle function which results in an elliptic locus, so it is likely that the latter requires a rational triangle function.

Related Work. Odehnal extensively studied loci of triangle centers over the poristic triangle family [19]. The early experimental result that the locus of the Incenter X_1 of billiard 3-periodics is an ellipse was subsequently proven [25, 7]. Proofs soon followed for the ellipticity of both X_2 [28] and X_3 [5, 7]; see Figures 16 and 15 in Appendix E. More recently, a theory for the ellipticity of a locus based on certain properties of a triangle is being developed, see [14]. For a textbook on Poncelet-based phenomena see [8].

Outline. Our main methods appear in Sections 2 and 3. We conclude in Section 4 with a list of questions and interesting links and videos. The Appendices contain supporting material. Most figures contain clickable links to relevant videos and/or the experiment displayed on our browser-based app [3].

2. DETECTING ELLIPTIC LOCI

Let the boundary of the EB be given by ($a > b > 0$):

$$(1) \quad f(x, y) = \left(\frac{x}{a}\right)^2 + \left(\frac{y}{b}\right)^2 = 1.$$

We describe a numerically-assisted method² which proves that the locus of a given triangle center is elliptic or otherwise. We then apply it to the first 100 triangle centers. listed in [16]. Indeed, a much larger list could be tested.

2.1. Proof Method. Our proof method consists of two phases, one numeric, and one symbolic, Figure 4. It makes use of the following Lemmas, whose proofs appear in Appendix D:

Lemma 1. *The locus of a triangle center X_i is symmetric about both EB axes and centered on the latter's origin.*

Proof. Given a 3-periodic $T = P_1P_2P_3$. Since the EB is symmetric about its axes, the family will contain the reflection of T about said axes, call these T' and T'' . Since triangle centers are invariant with respect to reflections, Appendix A, X'_i and X''_i will be found at similar reflected locations. \square

²We started with visual inspection, but this is both laborious and unreliable, some loci (take X_{30} and X_6 as examples) are indistinguishable from ellipses to the naked eye.

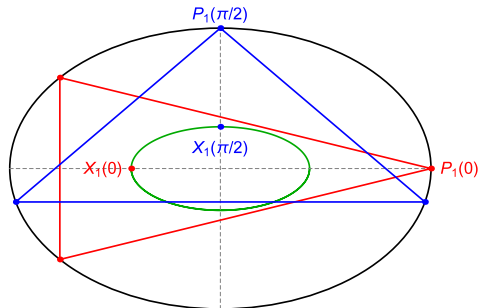


FIGURE 3. With P_1 at the right (resp. top) vertex of the EB, the orbit is a sideways (resp. upright) isosceles triangle, solid red (resp. solid blue). Not shown are their two symmetric reflections. Also shown (green) is the locus of a sample triangle center, X_1 in this case. At the isosceles positions, vertices will lie on the axis of symmetry of the triangle, Lemma 2. When the locus is elliptic, the x, y coordinates of $X_i(0), X_i(\pi/2)$ are the semi-axes a_i, b_i , respectively.

Note that if the locus is elliptic, the above implies it will be concentric and axis-aligned with the EB.

Lemma 2. *Any triangle center X_i of an isosceles triangle is on the axis of symmetry of said triangle.*

Lemma 3. *A parametric traversal of P_1 around the EB boundary triple covers the locus of triangle center X_i , elliptic or not.*

See Section 2.5 for more details.

A first phase fits a concentric, axis-aligned ellipse to a fine sampling of the locus of some triangle center X_i . A good fit occurs when the error is several orders of magnitude³ less than the sum of axes regressed by the process. False negatives are eliminated by setting the error threshold to numeric precision. False positives can be produced by adding arbitrarily small noise to samples of a perfect ellipse, though this type of misclassification does not survive the next, symbolic phase.

A second phase attempts to symbolically verify via a Computer Algebra System (CAS) if the parametric locus of the X_i satisfies the equation of a concentric, axis-aligned ellipse. Expressions for its semi-axes are obtained by evaluating X_i at isosceles orbit configurations, Figure 3. The method is explained in detail in Figure 5.

2.2. Phase 1: Least-Squares-Based Candidate Selection. Let the position of $X_i(t)$ be sampled (randomly or uniformly) at $t_k \in [0, 2\pi]$, $k = 1 \dots M$. If the locus is an ellipse, then the latter is concentric and axis-aligned with the EB, Lemma 1. Express the squared error as the sum of squared sample

³Robust fitting of ellipses to a cloud of points is not new [6]. In our case, the only source of error in triangle center coordinates is numerical precision, whose propagation can be bounded by Interval Analysis [18, 29].

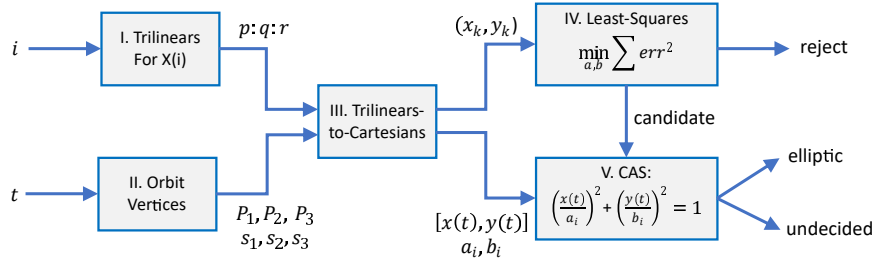


FIGURE 4. Our method as a flow-chart, modules labeled from I to V: (I) Once the i th center is specified, its trilinears $p : q : r$ (see Appendix A) are obtained from the Encyclopedia of triangle centers (ETC) [16]. (II) Given a symbolic parameter t or a numeric sample t_k , obtain cartesian coordinates for orbit vertices and the sidelengths, Appendix C.2. (III) Combine trilinears and orbit data to obtain, via (3), numeric cartesian coordinates for $X_i(t_k)$ or symbolically as $X_i(t)$. (IV) Least-squares fit an axis-aligned, concentric ellipse to the (x_k, y_k) samples and accept X_i as candidate if the fit error is sufficiently small. (V) Verify, via a Computer Algebra System (CAS), if the parametric locus $X_i(t)$ satisfies the equation of an ellipse whose axes a_i, b_i are obtained symbolically in II-III by setting $t = 0, \pi/2$. If the CAS is successful, $X_i(t)$ is deemed elliptic, otherwise the result is “undecided”. The CAS was successful for all 29 candidates selected by IV out of the first 100 Kimberling centers.

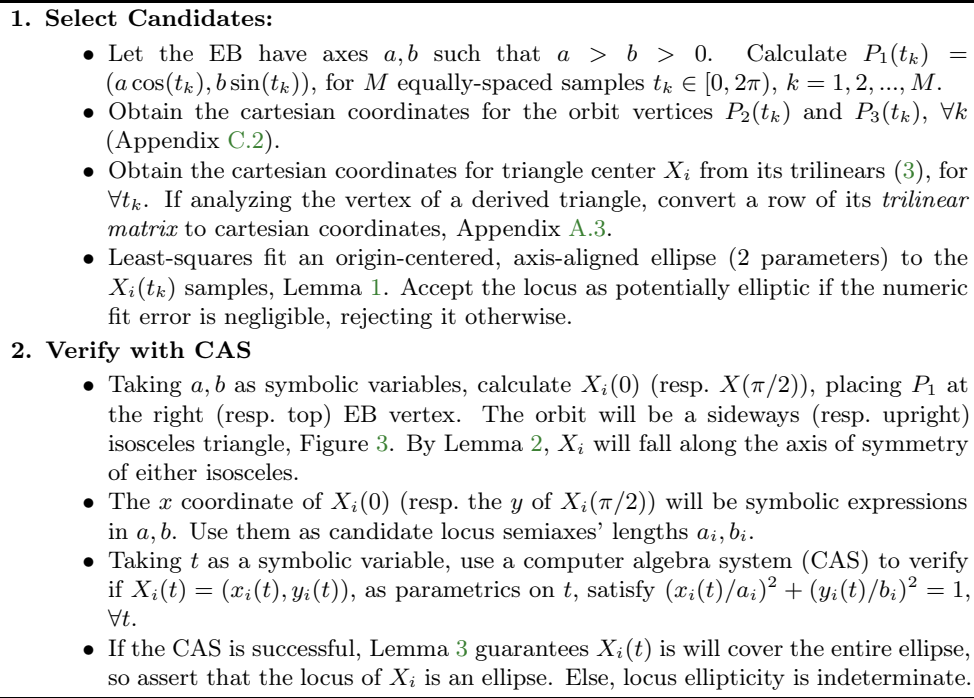


FIGURE 5. Method for detecting ellipticity of a triangle center locus.

deviations from an implicit ellipse:

$$\text{err}^2(a_i, b_i) = \sum_{k=1}^M \left[\left(\frac{x_k}{a_i} \right)^2 + \left(\frac{y_k}{b_i} \right)^2 - 1 \right]^2$$

Least-squares can be used to estimate the semi-axes:

$$(\hat{a}_i, \hat{b}_i) = \arg \min_{a,b} \{\text{err}^2(a_i, b_i)\}$$

The first 100 Kimberling centers separate into two distinct clusters: 29 with negligible least-squares error, and 71 with finite ones. These are shown in ascending order of error in our companion website [9, Part II].

A gallery of loci generated by X_1 to X_{100} (as well as vertices of several derived triangles) is provided in [20].

2.3. Phase 2: Symbolic Verification with a CAS. A CAS was successful in symbolically verifying that all 29 candidates selected in Phase 1 satisfy the equation of an ellipse (none were undecided). As an intermediate step, explicit expressions for their elliptic semi-axes were computed and appear in [9, Part I].

Theorem 1. *Out of the first 100 centers in [16], exactly 29 produce elliptic loci, all of which are concentric and axis-aligned with the EB. These are $X_{i,i=1, 2, 3, 4, 5, 7, 8, 10, 11, 12, 20, 21, 35, 36, 40, 46, 55, 57, 63, 65, 72, 78, 79, 80, 84, 88, 90}$. Specifically:*

- *The loci of $X_i, i = 2, 7, 57, 63$ are ellipses homothetic to the EB.*
- *The loci of $X_i, i = 4, 10, 40$ are ellipses homothetic to a 90° -rotated copy of the EB.*
- *The loci of $X_i, i = 88, 100$ are ellipses identical to the EB.*
- *The loci of X_{55} is an ellipse homothetic to the $N = 3$ caustic.*
- *The loci of $X_i, i = 3, 84$ are ellipses homothetic to a 90° -rotated copy of the $N = 3$ caustic.*
- *The locus of X_{11} is an ellipse identical to the $N = 3$ caustic.*

The above are summarized on Table 1. The least-square fit errors for the first 100 Kimberling are shown in Figure 6.

Remark 1. *The loci of $X_i, i = 1, 2, 3, 4$ are the ellipses $x^2/a_i^2 + y^2/b_i^2 = 1$. Via CAS, their semi-axes (a_i, b_i) are given by:*

$$\begin{aligned} a_1 &= \frac{\delta - b^2}{a} & b_1 &= \frac{a^2 - \delta}{b} \\ a_2 &= k_2 a & b_2 &= k_2 b \\ a_3 &= \frac{a^2 - \delta}{2b} & b_3 &= \frac{\delta - b^2}{2a} \\ a_4 &= \frac{k_4}{a} & b_4 &= \frac{k_4}{b} \end{aligned}$$

where $\delta^2 = a^4 + b^4 - a^2 b^2$, $k_2 = (2\delta - a^2 - b^2)/c^2$, $k_4 = [(a^2 + b^2)\delta - 2a^2 b^2]/c^2$, and $c^2 = a^2 - b^2$.

Explicit expressions for the locus semi-axes for abovementioned centers appear in [9, Part I].

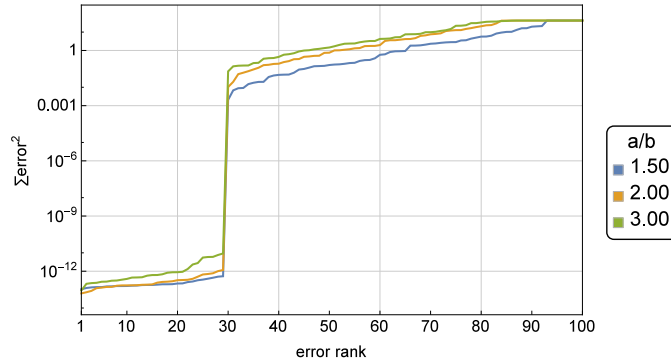


FIGURE 6. Log of Least-squares error for first 100 Kimberling centers in ascending order of error, for three values of a/b , $M = 1500$. Elliptic vs. non-elliptic centers are clearly separated in two groups whose errors differ by several orders of magnitude. A table in [9, Part II] shows that X_{37} and X_6 are ranks 30 and 31 respectively, i.e., they are the centers whose non-elliptic loci are closest to a perfect ellipse.

row	X_i	definition	sim	row	X_i	definition	sim
1	1	Incenter	J^t	16	46	X_4 -Ceva Conj. of X_1	
2	2	Barycenter	B	17	55	Insimilictr(Circumc.,Incir.)	C
3	3	Circumcenter	C^t	18	56	Exsimilictr(Circumc.,Incir.)	
4	4	Orthocenter	B^t	19	57	Isogonal Conj. of X_9	B
5	5	9-Point Center		20	63	Isogonal Conj. of X_{19}	B
6	7	Gergonne Point	B	21	65	Intouch Triangle's X_4	
7	8	Nagel Point		22	72	Isogonal Conj. of X_{28}	J
8	10	Spieker Center	B^t	23	78	Isogonal Conj. of X_{34}	
9	11	Feuerbach Point	C^+	24	79	Isogonal Conj. of X_{35}	
10	12	$\{X_{1,5}\}$ -Harm.Conj. of X_{11}		25	80	Refl. of X_1 about X_{11}	J^t
11	20	de Longchamps Point		26	84	Isogonal Conj. of X_{40}	C^t
12	21	Schiffler Point		27	88	Isogonal Conj. of X_{44}	B^+
13	35	$\{X_{1,3}\}$ -Harm.Conj. of X_{36}		28	90	X_3 -Cross Conj. of X_1	
14	36	Inverse-in-Circumc. of X_1		29	100	Anticomplement of X_{11}	B^+
15	40	Bevan Point	B^t				

TABLE 1. The 29 Kimberling centers within X_1 to X_{100} with elliptic loci. Under column “sim.”, letters B,C,J indicate the locus is similar to EB, caustic, or Excentral locus, respectively. An additional + (resp. t) exponent indicates the locus is identical (resp. similar to a perpendicular copy) to the indicated ellipse. Note: the ellipticity of $X_i, i = 1, 2, 3, 4$ was previously proven [25, 32, 5, 7].

2.4. The quartic locus of the Symmedian Point. The construction of the Symmedian point X_6 of a triangle is shown in Figure 7.

Over 3-periodic orbits in an EB with $a/b = 1.5$, the locus of X_6 is visually indistinguishable from an ellipse, Figure 8. Fortunately, its fit error is 10 orders of magnitude higher than the ones produced by true elliptic loci, see [9, Part II]. So it is easily rejected by the least-squares phase. Indeed, symbolic manipulation with a CAS yields:

Theorem 2. *The locus of X_6 is a convex quartic given by:*

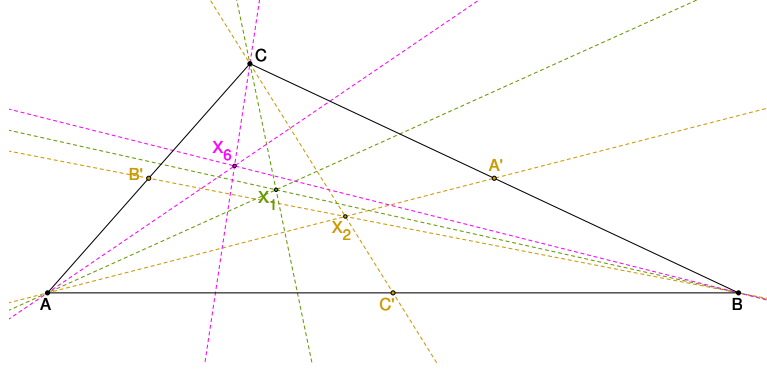


FIGURE 7. Given a triangle ABC , the Symmedian point X_6 is the point of concurrence of the three *symmedians* (pink), where the latter is a reflection of a median (brown) about the corresponding angular bisector (green). Medians (resp. angular bisectors) concur at the barycenter X_2 (resp. the incenter X_1).

$$\mathcal{X}_6(x, y) = c_1x^4 + c_2y^4 + c_3x^2y^2 + c_4x^2 + c_5y^2 = 0$$

where:

$$\begin{aligned} c_1 &= b^4(5\delta^2 - 4(a^2 - b^2)\delta - a^2b^2) & c_2 &= a^4(5\delta^2 + 4(a^2 - b^2)\delta - a^2b^2) \\ c_3 &= 2a^2b^2(a^2b^2 + 3\delta^2) & c_4 &= a^2b^4(3b^4 + 2(2a^2 - b^2)\delta - 5\delta^2) \\ c_5 &= a^4b^2(3a^4 + 2(2b^2 - a^2)\delta - 5\delta^2) & \delta &= \sqrt{a^4 - a^2b^2 + b^4} \end{aligned}$$

Proof. Using a CAS, obtain symbolic expressions for the coefficients of a quartic symmetric about both axes (no odd-degree terms), passing through 5 known-points. Still using a CAS, verify the symbolic parametric for the locus satisfies the quartic. \square

Note the above is also satisfied by a degenerate level curve $(x, y) = (0, 0)$, which we ignore.

Remark 2. The axis-aligned ellipse \mathcal{E}_6 with semi-axes a_6, b_6 is internally tangent to $\mathcal{X}_6(x, y) = 0$ at the four vertices where:

$$(2) \quad a_6 = \frac{[(3a^2 - b^2)\delta - (a^2 + b^2)b^2] a}{a^2b^2 + 3\delta^2}, \quad b_6 = \frac{[(a^2 - 3b^2)\delta + (a^2 + b^2)a^2] b}{a^2b^2 + 3\delta^2}$$

Table 2 shows the above coefficients numerically for a few values of a/b .

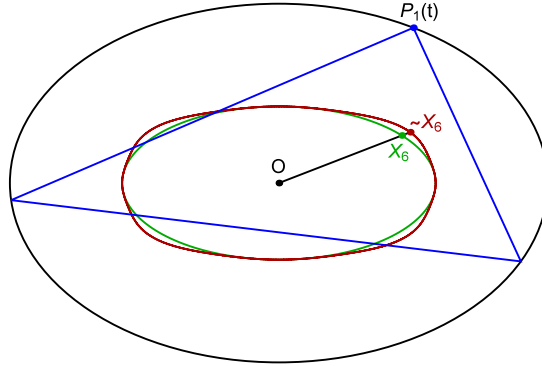


FIGURE 8. An $a/b = 1.5$ EB is shown (black) as well as a sample 3-periodic (blue). At this aspect ratio, the locus of X_6 (green) is indistinguishable to the naked eye from a perfect ellipse. To see it is non-elliptic, consider the locus of a point $\sim X_6(t) = X_6(t) + k|X_6(t) - Y_6'(t)|$, with $k = 2 \times 10^6$ and $Y_6'(t)$ the intersection of $OX_6(t)$ with a best-fit ellipse (visually indistinguishable from green), (2). [app](#)

a/b	a_6	b_6	c_1/c_3	c_2/c_3	c_4/c_3	c_5/c_3	$A(\mathcal{E}_6)/A(\mathcal{X}_6)$
1.25	0.433	0.282	0.211	1.185	-0.040	-0.095	0.9999
1.50	0.874	0.427	0.114	2.184	-0.087	-0.399	0.9998
2.00	1.612	0.549	0.052	4.850	-0.134	-1.461	0.9983
3.00	2.791	0.620	0.020	12.423	-0.157	-4.769	0.9949

TABLE 2. Coefficients c_i/c_3 , $i = 1, 2, 4, 5$ for the quartic locus of X_6 as well as the axes a_6, b_6 for the best-fit ellipse, for various values of a/b . The last-column reports the area ratio of the internal ellipse \mathcal{E}_6 (with axes a_6, b_6) to that of the quartic locus \mathcal{X}_6 , showing an almost exact match.

2.5. Locus Triple Winding. As an illustration of Lemma 3, consider the elliptic locus of X_1 , the Incenter⁴. Consider the locus of a point Y_1 located on between X_1 and an Intouchpoint I_1 , Figure 2 (left):

$$Y_1(t; \rho) = (1 - \rho)X_1(t) + \rho I_1(t), \quad \rho \in [0, 1]$$

When $\rho = 1$ (resp. 0), $Y_1(t)$ is the two-lobe locus of the Intouchpoints (resp. the elliptic locus of X_1). With ρ just above zero, Y_1 winds thrice around the EB center. At $\rho = 0$, the two lobes and the remainder of the locus become one and the same: Y_1 winds thrice over the locus of the Incenter, i.e., the latter is the limit of such a convex combination.

It can be shown that at $\rho = \rho^*$, with $\rho^* = 1 - (b/a)^2$, the two $Y_1(t)$ lobes touch at the the EB center. When $\rho > \rho^*$ (resp. $\rho < \rho^*$), the locus of $Y_1(t)$ has winding number 1 (resp. 3) with respect to the EB center, see Figure 9.

⁴The same argument is valid for the non-elliptic locus of, e.g., X_{59} , Figure 2 (right).

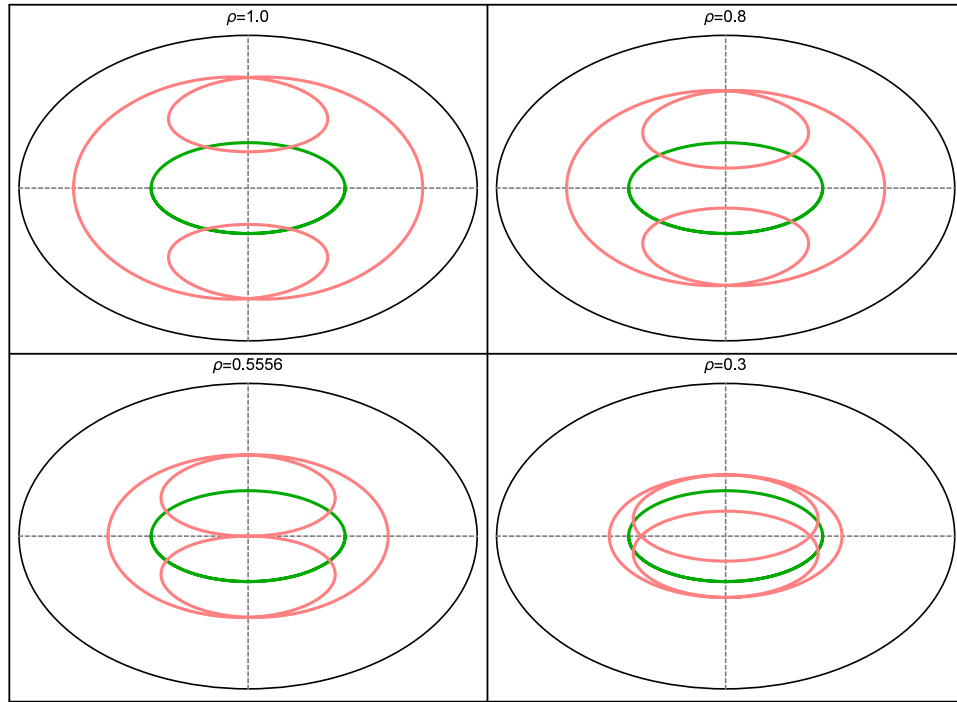


FIGURE 9. An $a/b = 1.5$ EB is shown (black) as well as the elliptic locus of X_1 (green) and the locus of $Y_1(t)$ (pink), the convex combination of $X_1(t)$ and an Intouchpoint given by a parameter $\rho \in [0, 1]$, see Figure 2(left). At $\rho = 1$ (top-left), $Y_1(t)$ is the two-lobe locus of the Intouchpoint. For every tour of an orbit vertex $P_1(t)$ around the EB, $Y_1(t)$ winds once over its locus. At $\rho = 0.8$ (top-right) the lobes approach each other but still lie in different half planes. At $\rho = \rho^* = 1 - (b/a)^2$, the lobes touch at the EB center (bottom-left). If $\rho \in (0, \rho^*)$, the two lobes self-intersect twice. As $\rho \rightarrow 0$, the two lobes become nearly coincidental (bottom-right). At $\rho = 0$, the Y_1 locus with its two lobes all collapse to the Incenter locus ellipse (green), in such a way that for every tour of $P_1(t)$ around the EB, X_1 winds thrice over its locus. [Video 1](#), [Video 2](#)

A similar phenomenon occurs for loci of convex combinations of the following pairs: (i) Barycenter X_2 and a side midpoint, (ii) Circumcenter X_3 and a side midpoint, (iii) Orthocenter X_4 and altitude foot, etc., see [21, pl#11,12].

3. TOWARD A TYPIFICATION OF LOCI

Our use of a few dozen centers listed in [16] was a means to validate our approach. In general we would like to predict locus type based on any triangle function, hand-curated or not. Below we take a few steps toward building a practical Computational Algebraic Geometry context useful for practitioners.

3.1. Trilinears: No Apparent Pattern. When one looks at a few examples of triangle centers whose loci are elliptic vs non, one finds no apparent algebraic pattern in said trilinears, Table 6 in Appendix A.1.

eqns.	description	zero set of
3	vertices on the EB	$(x_i/a)^2 + (y_i/b)^2 - 1, i = 1, 2, 3$
3	reflection law at P_j j, k, ℓ cyclic, $\mathcal{A} = \text{diag}(1/a^2; 1/b^2)$	$(\mathcal{A}P_j \cdot P_\ell - \mathcal{A}P_j \cdot P_j) P_k - P_j $ $-(\mathcal{A}P_j \cdot P_k - \mathcal{A}P_j \cdot P_j) P_\ell - P_j $
3	sidelengths	$(x_i - x_j)^2 + (y_i - y_j)^2 - s_k^2$
2	locus cartesians, (3)	$(ps_1 + qs_2 + rs_3)(x, y) - ps_1P_1 + qs_2P_2 + rs_3P_3$
3	trilinears (must rationalize)	$p - h(s_1, s_2, s_3); q - h(s_2, s_3, s_1); r - h(s_3, s_1, s_2)$

TABLE 3. System of 14 equations which the locus must satisfy. The three equations in the third line are obtained from the reflection law – angle of incidence equals the angle of reflection – imposed on the vertices of a triangular orbit.

A few observations include:

- The locus of a triangle center is symmetric about both EB axes, Lemma 1, Section 3.
- Some trilinear centers rational on the sidelengths which produce (i) elliptic loci (e.g., X_1, X_2 , etc.) as well as (ii) non-elliptic (e.g., X_6, X_{19} , etc.).
- No locus has been found with more than 6 intersections with a straight line, suggesting the degree is at most 6.
- No center has been found with non-rational trilinears whose locus is an ellipse⁵, suggesting that the locus of non-rational centers is always non-elliptic.

3.2. An Algebraic Ambient. Given EB semi-axes a, b , our problem can be described by the following 14 variables:

- 6 triangle vertex coordinates, $P_i = (x_i, y_i), i = 1, 2, 3$;
- 3 sidelengths s_1, s_2, s_3 ;
- 3 trilinears p, q, r ;
- 2 locus coordinates x, y .

These are related by the system of 14 polynomial equations defined in Table 3.

Since the 3-periodic family of orbits is one dimensional, out of the first 9 equations, one is functionally dependent on the rest. Therefore, we have 13 independent equations in 14 variables, yielding a 1d algebraic variety, which can be complexified if desired, as in [5, 10, 11, 25].

Can tools from computational Algebraic Geometry [27, 30] be used to eliminate 12 variables automatically, thus obtaining a single polynomial equation $\mathcal{L}(x, y) = 0$ whose Zariski closure contains the locus? Below we provide a method based on the theory of resultants [17, 30] to compute \mathcal{L} for a subset of triangle centers.

⁵Not shown, but also tested were non-rational triangle centers $X_j, j = 14, 16, 17, 18, 359, 360, 364, 365, 367$.

3.3. When Trilinears are Rational. Consider a triangle center X whose trilinears $p : q : r$ are rational on the sidelengths s_1, s_2, s_3 , i.e., the triangle center function h is rational, equation (4).

Theorem 3. *The locus of a rational triangle center is an algebraic curve.*

We thank one of the referees for kindly contributing the outline for this proof.

Proof. Consider the complexified variables of the first 4 rows of the table 3: the x_i, y_i and s_i . We have a 9 dimensional complex space. Consider the Zariski closure V in $\mathbb{P}_9\mathbb{C}$ of the complex algebraic subset defined by the 9 first equations given in the Table 3. Explicitly we have the equations:

$$\begin{aligned} f_i &= \frac{x_i^2}{a^2} + \frac{y_i^2}{b^2} - 1 = 0, \quad (i = 1, 2, 3) \\ f_4 &= \left(\frac{x_1x_2}{a^2} + \frac{y_1y_2}{b^2} - 1\right)s_2 - \left(\frac{x_1x_3}{a^2} + \frac{y_1y_3}{b^2} - 1\right)s_3 = 0 \\ f_5 &= \left(\frac{x_1x_2}{a^2} + \frac{y_1y_2}{b^2} - 1\right)s_1 - \left(\frac{x_2x_3}{a^2} + \frac{y_2y_3}{b^2} - 1\right)s_3 = 0 \\ f_6 &= \left(\frac{x_1x_3}{a^2} + \frac{y_1y_3}{b^2} - 1\right)s_1 - \left(\frac{x_2x_3}{a^2} + \frac{y_2y_3}{b^2} - 1\right)s_2 = 0 \\ f_7 &= (x_2 - x_1)^2 + (y_2 - y_1)^2 - s_3^2 = 0 \\ f_8 &= (x_2 - x_3)^2 + (y_2 - y_3)^2 - s_1^2 = 0 \\ f_9 &= (x_3 - x_1)^2 + (y_3 - y_1)^2 - s_2^2 = 0 \end{aligned}$$

By construction, it is a complex projective algebraic subset of $\mathbb{P}_9\mathbb{C}$. We have that $s_2f_5 - s_3f_6 - s_1f_4 = 0$. Computing its dimension it follows that:

- (i) the rank of the Jacobian matrix given by the 5 equations $f_1 = f_2 = f_3 = f_4 = f_5 = 0$ in relation to the variables $(x_1, y_1, x_2, y_2, x_3)$ or $(x_1, y_1, x_2, y_2, y_3)$ is generically 5.
- (ii) the rank of the Jacobian matrix given by the 9 equations is generically 8.
- (iii) the s_k are determined by the x_i, y_i (last 3 equations of Table 3) and that the set of complex triangular orbits is of dimension 1, see [5, 10, 11, 25], and [7] for an explicit parametrization of V . Longer (explicit) expressions appear in Appendix C.

This implies that V is a projective algebraic curve of $\mathbb{P}_9\mathbb{C}$, the complex projective space of dimension 9. The map which associates any point of V with $X = (x, y) \in \mathbb{P}_2\mathbb{C}$ as in Equation 3 (where p, q, r are given rational maps of the s_i) is well-defined and holomorphic on an algebraic open subset of V , and hence, on the complement of a discrete subset of V . Therefore, it is defined and holomorphic everywhere on V . Now its image is an analytic subset of $\mathbb{P}_2\mathbb{C}$ (Remmert proper mapping theorem) hence an algebraic subset (Chow theorem), see [13, Ch.V]. Its dimension is less or equal than 1, otherwise it would be the whole $\mathbb{P}_2\mathbb{C}$ (an impossibility, since it is bounded for real

points). When the dimension of the image is zero the locus degenerates to a point. \square

A typical example of a point-locus is that of the Mittenpunkt X_9 , which remains stationary at the center of the EB. In this case $p = h(s_1, s_2, s_3) = s_2 + s_3 - s_1$, $q = h(s_2, s_3, s_1) = s_1 + s_3 - s_2$ and $r = h(s_3, s_1, s_2) = s_1 + s_2 - s_3$. In the EB we have that $X_9 = (0, 0)$.

Proposition 1. *Over 3-periodics in the EB, the Mittenpunkt X_9 is the only triangle center whose locus is a point.*

Proof. Given the four-fold symmetry in the one-dimensional family of 3-periodics in the EB, the locus of any triangle center must be symmetric about both the vertical and horizontal semi-axes of the EB. So if some center's locus is a point, said point must be at the center of the EB. Over a continuous set of generic triangles (such as those in the 3-periodic family), two distinct triangle centers cannot always coincide (other than in a discrete set of configurations), so the claim follows. \square

3.4. Algorithm to compute the locus polynomial. Our algorithm is based on the following 3-steps which yield an algebraic curve $\mathcal{L}(x, y) = 0$ which contains the locus. We refer to Lemmas 4 and 5 appearing below. Appendix C contains supporting expressions.

Step 1. *Introduce the symbolic variables u, u_1, u_2 :*

$$u^2 + u_1^2 = 1, \quad \rho_1 u^2 + u_2^2 = 1.$$

The vertices will be given by rational functions of u, u_1, u_2

$$P_1 = (a u, b u_1), \quad P_2 = (p_{2x}, p_{2y})/q_2, \quad P_3 = (p_{3x}, p_{3y})/q_3$$

Expressions for P_1, P_2, P_3 appear in Appendix C as do equations $g_i = 0$, $i = 1, 2, 3$, polynomial in s_i, u, u_1, u_2 .

Step 2. *Express the locus X as a rational function on $u, u_1, u_2, s_1, s_2, s_3$.*

Convert $p : q : r$ to cartesian coordinates $X = (x, y)$ via Equation (3). From Lemma 4, it follows that (x, y) is rational on $u, u_1, u_2, s_1, s_2, s_3$.

$$x = \mathcal{Q}/\mathcal{R}, \quad y = \mathcal{S}/\mathcal{T}$$

To obtain the polynomials $\mathcal{Q}, \mathcal{R}, \mathcal{S}, \mathcal{T}$ on said variables $u, u_1, u_2, s_1, s_2, s_3$, one substitutes the p, q, r by the corresponding rational functions of s_1, s_2, s_3 that define a specific triangle center X . Other than that, the method proceeds identically.

Step 3. *Computing resultants. Our problem is now cast in terms of the polynomial equations:*

$$E_0 = \mathcal{Q} - x\mathcal{R} = 0, \quad F_0 = \mathcal{S} - y\mathcal{T} = 0$$

Firstly, compute the resultants, in chain fashion:

$$\begin{aligned} E_1 &= \text{Res}(g_1, E_0, s_1) = 0, & F_1 &= \text{Res}(g_1, F_0, s_1) = 0 \\ E_2 &= \text{Res}(g_2, E_1, s_2) = 0, & F_2 &= \text{Res}(g_2, F_1, s_2) = 0 \\ E_3 &= \text{Res}(g_3, E_2, s_3) = 0, & F_3 &= \text{Res}(g_3, F_2, s_3) = 0 \end{aligned}$$

It follows that $E_3(x, u, u_1, u_2) = 0$ and $F_3(y, u, u_1, u_2) = 0$ are polynomial equations. In other words, s_1, s_2, s_3 have been eliminated.

Now eliminate the variables u_1 and u_2 by taking the following resultants:

$$\begin{aligned} E_4(x, u, u_2) &= \text{Res}(E_3, u_1^2 + u^2 - 1, u_1) = 0 \\ F_4(y, u, u_2) &= \text{Res}(F_3, u_1^2 + u^2 - 1, u_1) = 0 \\ E_5(x, u) &= \text{Res}(E_4, u_2^2 + \rho_1 u^2 - 1, u_2) = 0 \\ F_5(y, u) &= \text{Res}(F_4, u_2^2 + \rho_1 u^2 - 1, u_2) = 0 \end{aligned}$$

This yields two polynomial equations $E_5(x, u) = 0$ and $F_5(y, u) = 0$.

Finally compute the resultant

$$\mathcal{L} = \text{Res}(E_5, F_5, u) = 0$$

that eliminates u and gives the implicit algebraic equation for the locus X .

Remark 3. *In practice, after obtaining a resultant, a human assists the CAS by factoring out spurious branches (when recognized), in order to get the final answer in more reduced form.*

When non-rational in the sidelengths, except a few cases (e.g., X_{359}, X_{360} which are transcendental), triangle centers in Kimberling's list have explicit trilinears involving fractional powers and/or terms containing the triangle area. Those can be made implicit, i.e, given by zero sets of polynomials involving p, q, r, s_1, s_2, s_3 . The chain of resultants to be computed will be increased by three, in order to eliminate the variables p, q, r before (or after) s_1, s_2, s_3 .

Lemma 4. *Let $P_1 = (au, b\sqrt{1-u^2})$. The coordinates of P_2 and P_3 of the 3-periodic billiard orbit are rational functions in the variables u, u_1, u_2 , where $u_1 = \sqrt{1-u^2}$, $u_2 = \sqrt{1-\rho_1 u^2}$ and $\rho_1 = c^4(b^2 + \delta)^2/a^6$.*

Proof. Follows directly from the parametrization of the billiard orbit, Appendix C.2. In fact, $P_2 = (x_2(u), y_2(u)) = (p_{2x}/q_2, p_{2y}/q_2)$ and $P_3 = (x_3(u), y_3(u)) = (p_{3x}/q_3, p_{3y}/q_3)$, where p_{2x}, p_{2y}, p_{3x} and p_{3y} have degree 4 in (u, u_1, u_2) and q_2, q_3 are algebraic of degree 4 in u . Expressions for u_1, u_2 appear in Appendix C.1. \square

Lemma 5. *Let $P_1 = (au, b\sqrt{1-u^2})$. Let s_1, s_2 and s_3 the sides of the triangular orbit $P_1P_2P_3$. Then $g_1(u, s_1) = 0$, $g_2(s_2, u_2, u) = 0$ and $g_3(s_3, u_2, u) = 0$ for polynomial functions g_i , defined in Appendix C.3.*

X_i	Name	Spurious Factors	Elliptic Factor	a_i	b_i
1	Incenter	very long expression	$[36(91 + 61\sqrt{61})x^2 + 324(139 + 19\sqrt{61})y^2 + 22761 - 3969\sqrt{61}]^6$	0.63504	0.29744
2	Barycenter	$(91500x^2 + 49922\sqrt{61} - 370993)^2$	$(100x^2 + 225y^2 + 52\sqrt{61} - 413)^3$	0.26205	0.1747
3	Circumcenter	$x(3600x^4 - 6380x^2 - 1539)(40x^2 + 5\sqrt{61} - 43)^2(-1104500y^2 + 591136\sqrt{61} - 4633685)^2(65880x^2 + 8527\sqrt{61} - 64649)^6$	$(5832x^2 + (2752 - 320\sqrt{61})y^2 + 5751 - 729\sqrt{61})^3$	0.099146	0.4763

TABLE 4. Method of Resultants applied to obtain the zero set for a few sample triangle centers with elliptic loci, for the specific case of $a/b = 1.5$. Both spurious and an elliptic factor are present. The latter are raised to powers multiple of three suggesting a phenomenon related to the triple cover, Section 2.5. Also shown are semi-axes a_i, b_i implied by the elliptic factor. These have been checked to be in perfect agreement with the values predicted for those semi-axes in [7].

Proof. Using the parametrization of the 3-periodic billiard orbit it follows that $s_1^2 - |P_2 - P_3|^2 = 0$ is a rational equation in the variables u, s_1 . Simplifying, leads to $g_1(s_1, u) = 0$.

Analogously for s_2 and s_3 . In this case, the equations $s_2^2 - |P_1 - P_3|^2 = 0$ and $s_3^2 - |P_1 - P_2|^2 = 0$ have square roots $u_2 = \sqrt{1 - \rho_1 u^2}$ and $u_1 = \sqrt{1 - u^2}$ and are rational in the variables s_2, u_2, u_1, u and s_3, u_2, u_1, u respectively. It follows that the degrees of g_1, g_2 , and g_3 are 10. Simplifying, leads to $g_2(s_2, u_2, u_1, u) = 0$ and $g_3(s_3, u_2, u_1, u) = 0$. \square

3.5. Examples. Table 4 shows the Zariski closure obtained contained the elliptic locus of a few triangle centers. Notice one factor is always of the form $[(x/a_i)^2 + (y/b_i)^2 - 1]^3$, related to the triple cover described in Section 2.5. The expressions shown required some manual simplification during the symbolic calculations.

4. CONCLUSION

A few interesting questions are posed to the reader.

- Can the degree of the locus of a triangle center or derived triangle vertex be predicted based on its trilinears?
- Is there a triangle center such that its locus intersects a straight line more than 6 times?
- Certain triangle centers have non-convex loci (e.g., X_{67} at $a/b = 1.5$ [20]). What determines non-convexity?
- What determines the number of self-intersections of a given locus?
- In the spirit of [5, 25], how would one determine via complex analytic geometry, that X_6 is a quartic?

id	Title	Section	youtu.be/<.>
01	Locus of X_1 is an Ellipse	1	BsyM7RnswA
02	Locus of Intouchpoints is non-elliptic	1, E	9xU6T7hQMzs
03	X_9 stationary at EB center	1	tMrBqfRBYik
04	Stationary Excentral Cosine Circle	1	ACinCf-D_0k
05	Loci for $X_1 \dots X_5$ are ellipses	E	sMcNzcYaqtg
06	Elliptic locus of Excenters similar to rotated X_1	E	Xxr1DUo19_w
07	Loci of X_{11} , X_{100} and Extouchpoints are the EB	E	TXdg7tU181c
08	Family of Derived Triangles	2	xyroRTEVNDc
09	Loci of Vertices of Derived Triangles	E,2	0GvCQbYqJyI
10	Peter Moses' 29 Billiard Points	2	JdcJt5PExsw
11	Convex Comb.: X_1 -Intouch and X_2 -Midpoint	2.5	3Gr3Nh5-jHs
12	Convex Comb.: X_3 -Midpoint and X_4 -Altfoot	2.5	HZFjkWD_CnE
13	Oval Locus of the Outer Napoleon Summits	4	70-E-NZrNCQ

TABLE 5. Videos mentioned in the paper available in a Youtube playlist [21]. The last column contains a clickable YouTube code.

- What is the non-elliptic locus described by the summits of equilaterals erected over each orbit side (used in the construction of the Outer Napoleon Triangle [33]). [21, pl#13]. What kind of curve is it?
- Within X_1 and X_{100} only X_i , $i = 13 \dots 18$ have irrational trilinears. X_j , $j = 359, 360$ are transcendental and X_k , $k = 364, 365, 367$ are irrational. In the latter two cases, the loci are numerically non-elliptic. Can any non-rational triangle center produce an ellipse?
- X_6 is the isogonal conjugate⁶ of X_2 . Though the latter's locus is an ellipse, the former's is a quartic. In the case of the isogonal pair X_3 and X_4 both are ellipses. What is the connection with isogonal (and/or isotomic⁷ transformations) and ellipticity?

4.1. **Videos and Media.** The reader is encouraged to browse our companion paper [22] where intriguing locus phenomena are investigated. Additionally, loci can be explored interactively with our browser-based app [3].

Videos mentioned herein are on a [playlist](#) [21], with links provided on Table 5.

ACKNOWLEDGMENTS

We warmly thank Clark Kimberling, Peter Moses, Sergei Tabachnikov, Richard Schwartz, Arseniy Akopyan, Olga Romaskevich, Ethan Cotterill, for their invaluable input during this research. We would like to thank the

⁶Given a point P , reflect the three P -cevians (lines through vertices and point P) about the angular bisectors. These meet at the *isogonal conjugate* of P .

⁷Given vertices P_i , $i = 1, 2, 3$, of a triangle and a point X , let Q_i denote the intersections of X -cevians with the opposite side. Let Q'_i be the reflection of Q_i about the midpoint of the corresponding side. Lines $P_iQ'_i$ meet at X' , the *isotomic conjugate* of X .

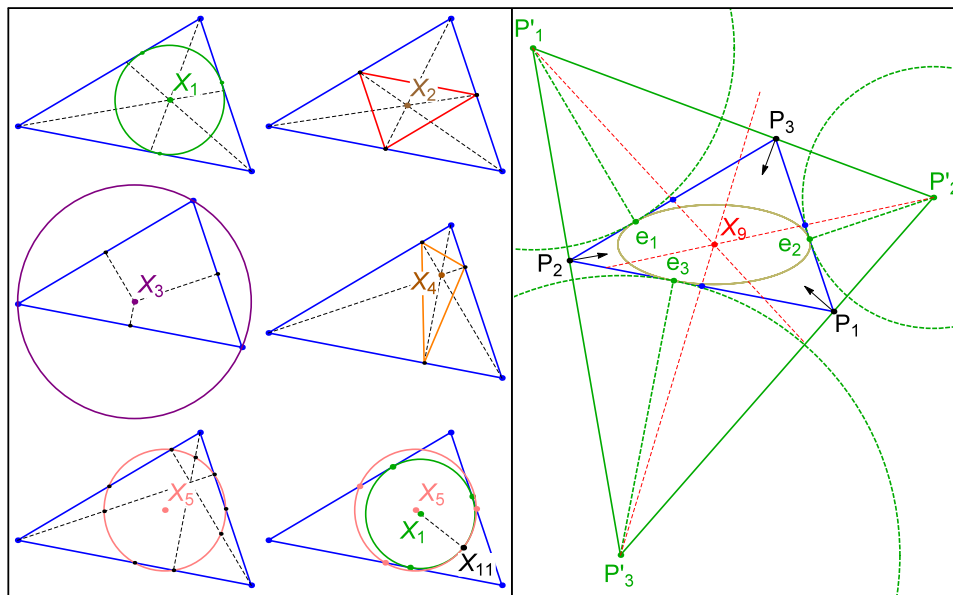


FIGURE 10. Constructions for triangle centers X_i , $i = 1, 2, 3, 4, 5, 9, 11$, taken from [23].

referees for all very useful suggestions, including an alternative proof for Theorem 3.

The first author is fellow of CNPq and coordinator of Project PRONEX/CNPq/ FAPEG 2017 10 26 7000 508.

APPENDIX A. TRIANGLE CENTERS

A.1. Triangle Centers. Constructions for a few basic triangle centers are shown in Figure 10, using Kimberling's X_i notation [16].

- The Incenter X_1 is the intersection of angular bisectors, and center of the Incircle (green), a circle tangent to the sides at three *Intouch-points* (green dots), its radius is the *Inradius* r .
- The Barycenter X_2 is where lines drawn from the vertices to opposite sides' midpoints meet. Side midpoints define the *Medial Triangle* (red).
- The Circumcenter X_3 is the intersection of perpendicular bisectors, the center of the *Circumcircle* (purple) whose radius is the *Circumradius* R .
- The Orthocenter X_4 is where altitudes concur. Their feet define the *Orthic Triangle* (orange).
- X_5 is the center of the 9-Point (or Euler) Circle (pink): it passes through each side's midpoint, altitude feet, and Euler points [33].
- The Feuerbach Point X_{11} is the single point of contact between the Incircle and the 9-Point Circle.

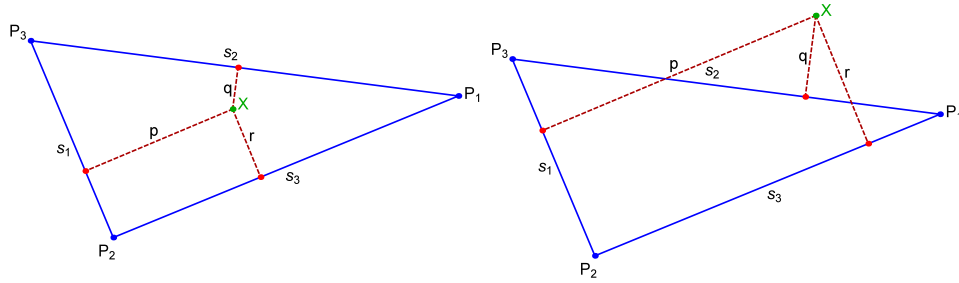


FIGURE 11. Trilinear coordinates $p : q : r$ for a point X on the plane of a generic triangle $T = P_1P_2P_3$ are homogeneous signed distances to each side whose lengths are s_1, s_2, s_3 . The red dots are known as the *pedal points* of X [33]. The left (resp. right) figure shows an interior (resp. exterior) point. In both cases p, r are positive however q is positive (resp. negative) in the former (resp. latter) case.

- Given a reference triangle $P_1P_2P_3$ (blue), the *Excenters* $P'_1P'_2P'_3$ are pairwise intersections of lines through the P_i and perpendicular to the bisectors. This triad defines the *Excentral Triangle* (green).
- The *Excircles* (dashed green) are centered on the Excenters and are touch each side at an *Extouch Point* $e_i, i = 1, 2, 3$.
- Lines drawn from each Excenter through sides' midpoints (dashed red) concur at the *Mittenpunkt* X_9 .
- Also shown (brown) is the triangle's *Mandart Inellipse*, internally tangent to each side at the e_i , and centered on X_9 . This is identical to the $N = 3$ caustic.

A.2. Trilinear Coordinates. Trilinear coordinates are signed distances to the sides of a triangle $T = P_1P_2P_3$, i.e. they are invariant with respect to similarity/reflection transformations, see Figure 11.

Trilinears can be easily converted to cartesian coordinates using [33]:

$$(3) \quad X = \frac{ps_1P_1 + qs_2P_2 + rs_3P_3}{ps_1 + qs_2 + rs_3}$$

where $s_1 = |P_3 - P_2|$, $s_2 = |P_1 - P_3|$ and $s_3 = |P_2 - P_1|$ are the sidelengths, Figure 11. For instance, the trilinears for the barycenter are $p = s_1^{-1}$, $q = s_2^{-1}$, $r = s_3^{-1}$, yielding the familiar $X_2 = (P_1 + P_2 + P_3)/3$.

A *triangle center* is such a triple obtained by applying a *triangle center function* h thrice to the sidelengths s_1, s_2, s_3 cyclically [15]:

$$(4) \quad p : q : r \iff h(s_1, s_2, s_3) : h(s_2, s_3, s_1) : h(s_3, s_1, s_2)$$

h must (i) be *bi-symmetric*, i.e., $h(s_1, s_2, s_3) = h(s_1, s_3, s_2)$, and (ii) homogeneous, $h(ts_1, ts_2, ts_3) = t^n h(s_1, s_2, s_3)$ for some n [15].

See Table 6 for triangle center functions for selected centers. Trilinears can be converted to cartesian coordinates using (3).

Trilinear coordinates for selected triangle centers appear in Table 6.

center	name	$h(s_1, s_2, s_3)$
X_1	Incenter	1
X_2	Barycenter	$1/s_1$
X_3	Circumcenter	$s_1(s_2^2 + s_3^2 - s_1^2)$
X_4	Orthocenter	$1/[s_1(s_2^2 + s_3^2 - s_1^2)]$
X_5	9-Point Center	$s_2 s_3 [s_1^2 (s_2^2 + s_3^2) - (s_2^2 - s_3^2)^2]$
X_{11}	Feuerbach Point	$s_2 s_3 (s_2 + s_3 - s_1)(s_2 - s_3)^2$
X_{88}	Isog. Conjug. of X_{44}	$1/(s_2 + s_3 - 2s_1)$
X_{100}	Anticomplement of X_{11}	$1/(s_2 - s_3)$
X_6	Symmedian Point	s_1
X_{13}^*	Fermat Point	$s_1^4 - 2(s_2^2 - s_3^2)^2 + s_1^2(s_2^2 + s_3^2 + 4\sqrt{3}A)$
X_{15}^*	2nd Isodynamic Point	$s_1[\sqrt{3}(s_1^2 - s_2^2 - s_3^2) - 4A]$
X_{19}	Clawson Point	$1/(s_2^2 + s_3^2 - s_1^2)$
X_{37}	Crosspoint of X_1, X_2	$s_2 + s_3$
X_{59}	Isog. Conj. of X_{11}	$1/[s_2 s_3 (s_2 + s_3 - s_1)(s_2 - s_3)^2]$
X_9	Mittelpunkt	$s_2 + s_3 - s_1$

TABLE 6. Triangle center function h for a few selected X_i 's, taken from [16]. The first 8 centers produce elliptic loci, whereas the remainder (**boldfaced**) do not. X_{13} and X_{15} are *starred* to indicate their trilinears are irrational: these contain A , the area the triangle, known (e.g., from Heron's formula) to be irrational on the sidelengths. We haven't yet detected an algebraic pattern which differentiates both groups, nor have we detected an irrational center whose locus is elliptic. Regarding the last row, the Mittenpunkt, we don't consider its locus to be elliptic since it degenerates to a point at the EB center.

A.3. Derived Triangles. A *derived triangle* T' is constructed from vertices of a reference triangle T . These can be represented as a 3x3 matrix, where each row, taken as trilinears, is a vertex of T' . For example, the Excentral, Medial, and Intouch Triangles T'_{exc} , T'_{med} , and T'_{int} are given by [33]:

$$\begin{bmatrix} -1 & 1 & 1 \\ 1 & -1 & 1 \\ 1 & 1 & -1 \end{bmatrix}, \begin{bmatrix} 0 & s_2^{-1} & s_3^{-1} \\ s_1^{-1} & 0 & s_3^{-1} \\ s_1^{-1} & s_2^{-1} & 0 \end{bmatrix}, \begin{bmatrix} 0 & \frac{s_1 s_3}{s_1 - s_2 + s_3} & \frac{s_1 s_2}{s_1 + s_2 - s_3} \\ \frac{s_2 s_3}{-s_1 + s_2 + s_3} & 0 & \frac{s_1 s_2}{s_1 + s_2 - s_3} \\ \frac{s_2 s_3}{-s_1 + s_2 + s_3} & \frac{s_1 s_3}{s_1 - s_2 + s_3} & 0 \end{bmatrix}$$

A few derived triangles are shown in Figure 12, showing a property similar to Lemma 2, Appendix D, namely, when the 3-periodic is an isosceles, one vertex of the derived triangle lies on the orbit's axis of symmetry.

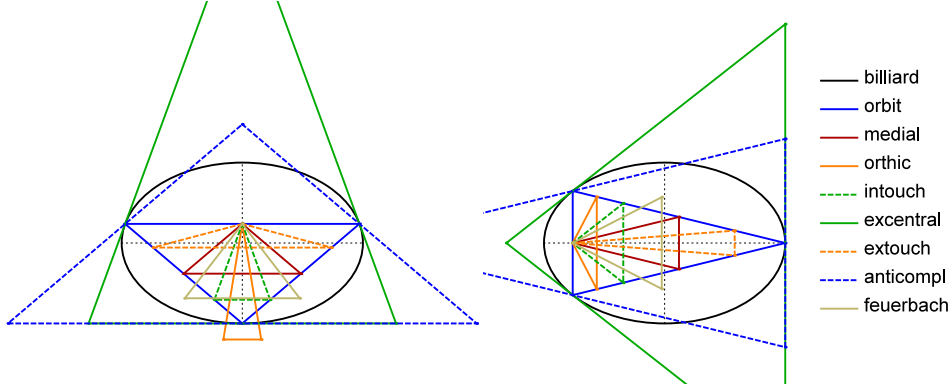


FIGURE 12. When the orbit is an isosceles triangle (solid blue), any derived triangle will contain one vertex on the axis of symmetry of the orbit. [Video](#)

APPENDIX B. REVIEW: ELLIPTIC BILLIARDS

An Elliptic Billiard (EB) is a particle moving with constant velocity in the interior of an ellipse, undergoing elastic collisions against its boundary [26, 31], Figure 13. For any boundary location, a given exit angle (e.g., measured from the normal) may give rise to either a quasi-periodic (never closes) or N -periodic trajectory [31], where N is the number of bounces before the particle returns to its starting location. All trajectory segments are tangent to a confocal caustic [31]. The EB is a special case of *Poncelet's Porism* [4]: if one N -periodic trajectory can be found departing from some boundary point, any other such point will initiate an N -periodic, i.e., a 1d *family* of such orbits will exist. A classic result is that N -periodics conserve perimeter [31].

APPENDIX C. EXPRESSIONS USED IN SECTION 3.3

Let the boundary of the Billiard satisfy Equation (1). Assume, without loss of generality, that $a \geq b$. Here we provide expressions used in Section 3. Let P_1, P_2, P_3 be an orbit's vertices.

C.1. Exit Angle Required for 3-Periodicity. Consider a starting point $P_1 = (x_1, y_1)$ on a Billiard with semi-axes a, b . The cosine of the exit angle α (measured with respect to the normal at P_1 , i.e., $\alpha = \theta_1/2$) required for the trajectory to close after 3 bounces is given by [7]:

$$\cos^2 \alpha = \frac{d_1^2 \delta_1^2}{d_2} = k_1, \quad \sin \alpha \cos \alpha = \frac{\delta_1 d_1^2}{d_2} \sqrt{d_2 - d_1^4 \delta_1^2} = k_2$$

with $c^2 = a^2 - b^2$, $d_1 = (ab/c)^2$, $d_2 = b^4 x_1^2 + a^4 y_1^2$, $\delta = \sqrt{a^4 + b^4 - a^2 b^2}$, and $\delta_1 = \sqrt{2\delta - a^2 - b^2}$.

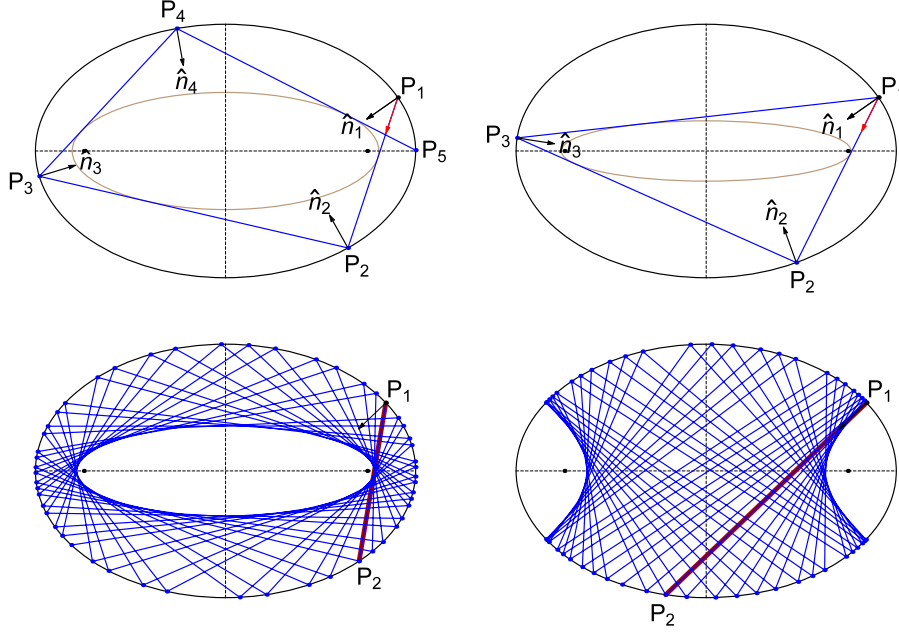


FIGURE 13. Trajectory regimes in an Elliptic Billiard, taken from [23]. **Top left**: first four segments of a trajectory departing at P_1 and toward P_2 , bouncing at $P_i, i = 2, 3, 4$. At each bounce the normal \hat{n}_i bisects incoming and outgoing segments. Joachimsthal's integral [31] means all segments are tangent to a confocal *caustic* (brown). **Top right**: a 3-periodic trajectory. All 3-periodics in this Billiard will be tangent to a special confocal caustic (brown). **Bottom**: first 50 segments of a non-periodic trajectory starting at P_1 and directed toward P_2 . Segments are tangent to a confocal ellipse (left) or hyperbola (right). The former (resp. latter) occurs if P_1P_2 passes outside (resp. between) the EB's foci (black dots).

C.2. Orbit Vertices. Given a starting vertex $P_1 = (x_1, y_1)$ on the EB, $P_2 = (p_{2x}, p_{2y})/q_2$, and $P_3 = (p_{3x}, p_{3y})/q_3$ where [7]:

$$\begin{aligned}
 p_{2x} &= -b^4 \left((a^2 + b^2) k_1 - a^2 \right) x_1^3 - 2a^4 b^2 k_2 x_1^2 y_1 \\
 &\quad + a^4 \left((a^2 - 3b^2) k_1 + b^2 \right) x_1 y_1^2 - 2a^6 k_2 y_1^3 \\
 p_{2y} &= 2b^6 k_2 x_1^3 + b^4 \left((b^2 - 3a^2) k_1 + a^2 \right) x_1^2 y_1 \\
 &\quad + 2a^2 b^4 k_2 x_1 y_1^2 - a^4 \left((a^2 + b^2) k_1 - b^2 \right) y_1^3 \\
 q_2 &= b^4 \left(a^2 - c^2 k_1 \right) x_1^2 + a^4 \left(b^2 + c^2 k_1 \right) y_1^2 - 2a^2 b^2 c^2 k_2 x_1 y_1 \\
 p_{3x} &= b^4 \left(a^2 - (b^2 + a^2) \right) k_1 x_1^3 + 2a^4 b^2 k_2 x_1^2 y_1 \\
 &\quad + a^4 \left(k_1 (a^2 - 3b^2) + b^2 \right) x_1 y_1^2 + 2a^6 k_2 y_1^3 \\
 p_{3y} &= -2b^6 k_2 x_1^3 + b^4 \left(a^2 + (b^2 - 3a^2) k_1 \right) x_1^2 y_1 \\
 &\quad - 2a^2 b^4 k_2 x_1 y_1^2 + a^4 \left(b^2 - (b^2 + a^2) k_1 \right) y_1^3, \\
 q_3 &= b^4 \left(a^2 - c^2 k_1 \right) x_1^2 + a^4 \left(b^2 + c^2 k_1 \right) y_1^2 + 2a^2 b^2 c^2 k_2 x_1 y_1.
 \end{aligned}$$

C.3. Polynomials Satisfied by the Sidelengths. Let sidelengths $s_1 = |P_3 - P_2|$, $s_2 = |P_1 - P_3|$, $s_3 = |P_2 - P_1|$. The following are polynomial expressions on s_i and u, u_1, u_2 :

$$\begin{aligned}
g_1 &= -h_1 s_1^2 + h_0, \quad g_2 = -h_1 s_2^2 - h_2 u_1 u_2 + h_3, \quad g_3 = -h_1 s_3^2 + h_2 u_1 u_2 + h_3 \\
h_0 &= 12c^{12}(a^2 + b^2 + 2\delta)u^8 + 24c^{10}(a^2b^2 + 2b^4 - 2\delta c^2u^6 \\
&\quad - 4c^4[10a^{10} - 12a^8b^2 + 11a^6b^4 - 7a^4b^6 + 24a^2b^8 - 8b^{10} \\
&\quad - (2(4a^4 - 2a^2b^2 + b^4))(a^4 - 2a^2b^2 + 4b^4)\delta]u^4 \\
&\quad + 8a^6c^2[4a^6 - 7a^4b^2 + 11a^2b^4 - 2b^6 - (2(a^2 + ab + b^2))(a^2 - ab + b^2)\delta]u^2 \\
&\quad + 4a^{12}\delta_1^2 \\
h_1 &= c^2(3c^4u^4 - 2c^2(a^2 - 2b^2u^2 - a^4))^2 \\
h_2 &= -2a(b^2 - \delta)\delta_1 u((3c^6\delta + (6(a^2 + b^2))c^6)u^6 + ((3(a^2 + 4b^2))c^4\delta \\
&\quad - (3(2a^4 - a^2b^2 - 4b^4))c^4)u^4 + ((b_2 - a^2)(7a^4 - 8b^4)\delta \\
&\quad + 2c^2(a^2 - 2b^2)(a^4 - 2b^4))u^2 + a^4(a^2 - 4b^2)\delta - a^4(2a^4 - 3a^2b^2 + 4b^4)) \\
h_3 &= c^6(9c^6u^{10} + 1)((18(a^4 + b^4))\delta - (3(7a^6 - 16a^4b^2 + 29a^2b^4 - 8b^6))u^8 \\
&\quad + 2c^2[(13a^8 - 12a^6b^2 + 49a^4b^4 - 54a^2b^6 + 16b^8) \\
&\quad - 2(10a^6 - 7a^4b^2 + 11a^2b^4 - 8b^6)\delta]u^6 \\
&\quad + ((28a^4\delta^2 - 40a^2b^6 + 16b^8)\delta - 26a^{10} + 12a^8b^2 + 42a^4b^6 - 48a^2b^8 + 16b^{10})u^4 \\
&\quad + a(13a^6 - 9a^4b^2 - 8b^4c^2 - (4(2a^4 + a^2b^2 - 2b^4))\delta)^4u^2 + 2a^8(\delta - a^8c^2)
\end{aligned}$$

APPENDIX D. PROOF OF LEMMAS USED IN SECTION 2

Lemma (3). *A parametric traversal of P_1 around the EB boundary is a triple cover of the locus of a triangle center X_i .*

Proof. Let $P_1(t) = (a \cos t, b \sin t)$. Let t^* (resp. t^{**}) be the value of t for which the 3-periodic orbit is an isosceles with a horizontal (resp. vertical) axis of symmetry, Figure 14, $t^* > t^{**}$. For such cases one can easily derive⁸:

$$\tan t^* = \frac{b\sqrt{2\delta - a^2 + 2b^2}}{a^2}, \quad \tan t^{**} = \frac{\sqrt{2\delta - 2a^2 + b^2}}{\sqrt{3}a}$$

with $\delta = \sqrt{a^4 - a^2b^2 + b^4}$ as above. Referring to Figure 14:

Affirmation 1. *A continuous counterclockwise motion of $P_1(t)$ along the intervals $[-t^*, -t^{**})$, $[-t^{**}, 0)$, $[0, t^{**})$, and $[t^{**}, t^*)$ will each cause X_i to execute a quarter turn along its locus, i.e., with t varying from $-t^*$ to t^* , X_i will execute one complete revolution on its locus⁹.*

Affirmation 2. *A continuous counterclockwise motion of $P_1(t)$ in the $[t^*, \pi - t^*)$ (resp. $[\pi - t^*, \pi + t^*)$, and $[\pi + t^*, 2\pi - t^*)$), visits the same 3-periodics as when t sweeps $[-t^*, -t^{**})$ (resp. $[-t^*, t^*)$, and $[t^*, \pi - t^*)$).*

⁸Indeed, $\sin t^* = Jb$ and $\cos t^{**} = Ja$, where J is Joachmisthal's constant ($N = 3$) [31].

⁹The direction of this revolution depends on X_i and its not always monotonic. The observation is valid for elliptic or non-elliptic loci alike. See [14] for details.

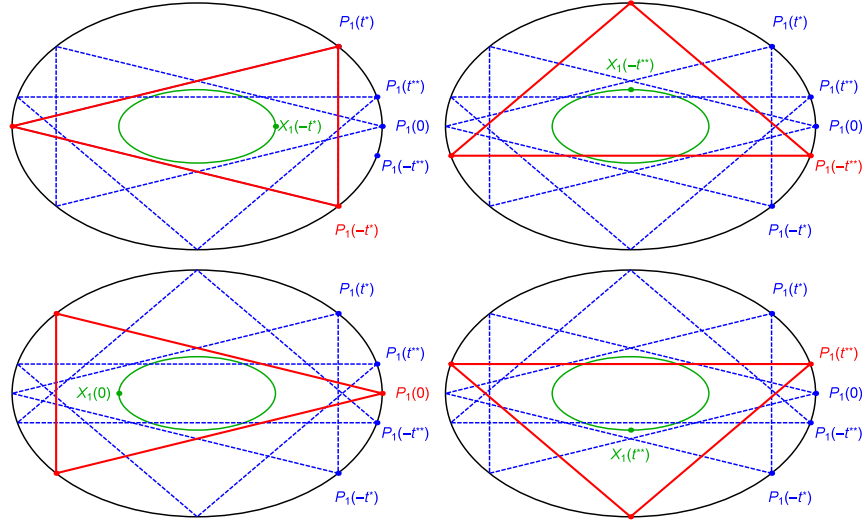


FIGURE 14. Counterclockwise motion of $P_1(t)$, for $t = [-t^*, t^*]$ can be divided in four segments delimited by $t = (-t^*, -t^{**}, 0, t^{**}, t^*)$. Orbit positions for the first four are shown (red polygons) in the top-left, top-right, bot-left, and bot-right pictures. At $P_1(\pm t^*)$ (resp. $P_1(\pm t^{**})$) the orbit is an isosceles triangle with a horizontal (resp. vertical) axis of symmetry. Observations 1,2 assert that a counterclockwise motion of $P_1(t)$ along each of the four intervals causes a triangle center X_i to execute a quarter turn along its locus (elliptic or not), and that a complete revolution of $P_1(t)$ around the EB causes X_i to wind thrice on its locus. For illustration, the locus of $X_1(t)$ is shown (green) at each of the four interval endpoints.

Therefore, a complete turn of $P_1(t)$ around the EB visits the 3-periodic family thrice, i.e., X_i will wind thrice over its locus. \square

Below we provide proofs of Lemmas 2, 1 and 3.

Lemma (2). *Any triangle center X_i of an isosceles triangle is on the axis of symmetry of said triangle.*

Proof. Consider a sideways isosceles triangle with vertices $P_1 = (x_1, 0)$, $P_2 = (-x_2, y_2)$ and $P_3 = (-x_2, -y_2)$, i.e., its axis of symmetry is the x axis. Let X_i have trilinears $p : q : r = h(s_1, s_2, s_3) : h(s_2, s_3, s_1) : h(s_3, s_1, s_2)$. Its cartesian coordinates are given by Equation (3). As $s_2 = s_3$ and h is symmetric on its last two variables $h(s_1, s_2, s_3) = h(s_1, s_3, s_2)$ it follows from equation (3) that $y_i = 0$. \square

Lemma (1). *If the locus of triangle center X_i is elliptic, said ellipse must be concentric and axis-aligned with the EB.*

Proof. This follows from Lemma 1. \square

Lemma (3). *If the locus of X_i is an ellipse, when $P_1(t)$ is at either EB vertex, its non-zero coordinate is equal to the corresponding locus semi-axis length.*

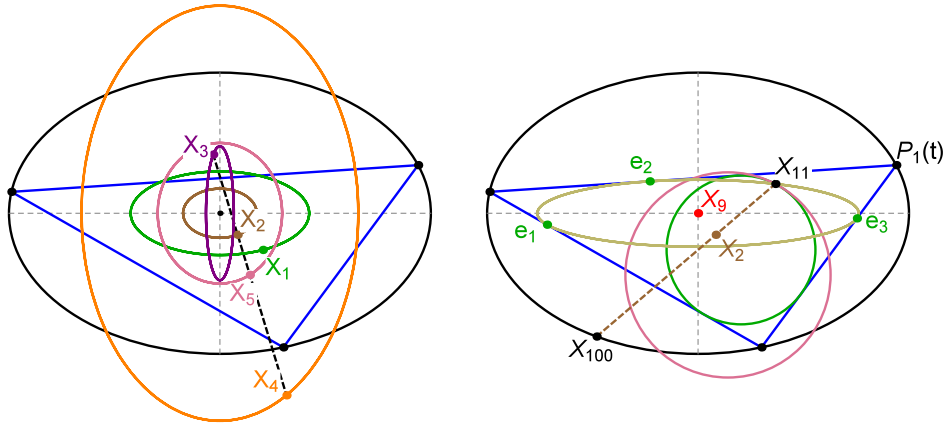


FIGURE 15. **Left:** The loci of Incenter X_1 , Barycenter X_2 , Circumcenter X_3 , Orthocenter X_4 , and center of the 9-Point Circle X_5 are all ellipses, [Video](#), [app](#). Also shown is the *Euler Line* (dashed black) which for any triangle, passes through all of X_i , $i = 1 \dots 5$ [33]. **Right:** A 3-periodic orbit starting at $P_1(t)$ is shown (blue). The locus of X_{11} , where the Incircle (green) and 9-Point Circle (pink) meet, is the caustic (brown), also swept by the Extouchpoints e_i . X_{100} (double-length reflection of X_{11} about X_2) is the EB [Video](#), [app](#).

Proof. The family of 3-periodic orbits contains four isosceles triangles, Figure 3. Parametrize $P_1(t) = (a \cos t, b \sin t)$. It follows from Lemma 1 that $X_i(0) = (\pm a_i, 0)$, $X_i(\pi/2) = (0, \pm b_i)$, $X_i(\pi) = (\mp a_i, 0)$ and $X_i(3\pi/2) = (0, \mp b_i)$, for some a_i, b_i . This ends the proof. \square

APPENDIX E. REVIEW: EARLY OBSERVATIONS

Figure 15 (left) shows the elliptic loci of X_k , $k = 1, \dots, 5$. The latter two are new results.

We have also observed that the locus of the Feuerbach Point X_{11} coincides with the $N = 3$ caustic, a confocal ellipse to which the 3-periodic family is internally tangent, Appendix B. Additionally, the locus of X_{100} , the anticomplement¹⁰ of X_{11} is the EB boundary. These phenomena appear in Figure 15 (right).

Indeed, some these facts will be known to triangle specialists if one regards the EB as the circumellipse centered on the Mittenpunkt X_9 [16, X(9)] and [12]. For example, a full 57 triangle centers lie on said circumellipse. An animation of some of these points is viewable in [21, pl#10].

Additionally, a few observations have been made [23] about the loci of vertices of orbit-derived triangles (see Appendix A.3), some of which are elliptic and others non, illustrated in Figure 16.

REFERENCES

- [1] Akopyan, A., Schwartz, R., Tabachnikov, S. (2020). Billiards in ellipses revisited. *Eur. J. Math.* doi.org/10.1007/s40879-020-00426-9.

¹⁰Double-length reflection about the Barycenter X_2 .

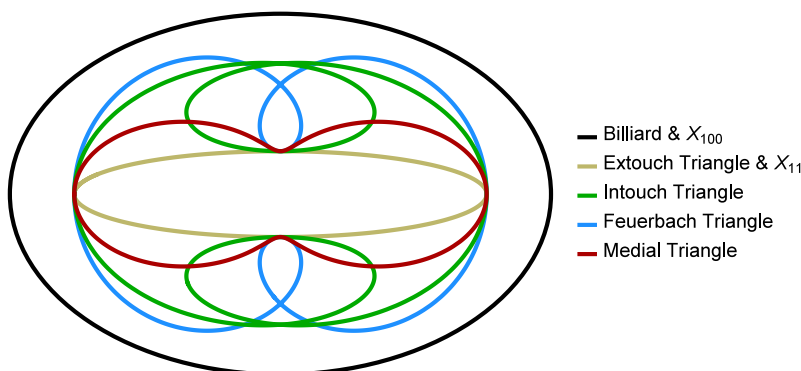


FIGURE 16. Loci generated by the vertices of selected orbit-derived triangles, namely: the Intouch (green), Feuerbach (blue, not to be confused with the Feuerbach *Point* X_{11}), and Medial (red) Triangles are non-elliptic. However, those of the Extouch Triangle (brown), are identical to the $N = 3$ caustic (a curve also swept by X_{11}). Not shown is the locus of the Excentral Triangle, an ellipse similar to a rotated copy of the Incenter locus. [app](#), [Video 1](#), [Video 2](#), [Video 3](#), [Video 4](#).

- [2] Bialy, M., Tabachnikov, S. (2020). Dan Reznik’s identities and more. *Eur. J. Math.* doi.org/10.1007/s40879-020-00428-7.
- [3] Darlan, I., Reznik, D. (2020). Ellipse mounted triangles. GitHub Pages. dan-reznik.github.io/ellipse-mounted-loci-p5js/.
- [4] Dragović, V., Radnović, M. (2011). *Poncelet Porisms and Beyond: Integrable Billiards, Hyperelliptic Jacobians and Pencils of Quadrics*. Frontiers in Mathematics. Basel: Springer.
- [5] Fierobe, C. (2021). On the circumcenters of triangular orbits in elliptic billiard. *J. Dyn. Control Syst.*, 27(4): 693–705.
- [6] Fitzgibbon, A., Pilu, M., Fisher, R. (1999). Direct least-square fitting of ellipses. *Pattern Analysis and Machine Intelligence*, 21(5).
- [7] Garcia, R. (2019). Elliptic billiards and ellipses associated to the 3-periodic orbits. *Amer. Math. Monthly*, 126(06): 491–504.
- [8] Garcia, R., Reznik, D. (2021). *Discovering Poncelet Invariants in the Plane*. Rio de Janeiro: IMPA.
- [9] Garcia, R., Reznik, D., Koiller, J. (2021). Companion website to “loci of 3-periodics in an elliptic billiard: Why so many ellipses?”. GitHub Pages. dan-reznik.github.io/why-so-many-ellipses/.
- [10] Glutsyuk, A. (2014). On quadrilateral orbits in complex algebraic planar billiards. *Moscow Math. J.*, 14(2): 239–289, 427.
- [11] Griffiths, P., Harris, J. (1978). On Cayley’s explicit solution to Poncelet’s porism. *Enseign. Math. (2)*, 24(1-2): 31–40.
- [12] Grozdev, S., Dekov, D. (2014). The computer program “Discoverer” as a tool of mathematical investigation. *Intl. J. of Comp. Disc. Math. (IJCDM)*. www.ddekov.eu/j/2014/JCGM201405.pdf.
- [13] Gunning, R. C., Rossi, H. (1965). *Analytic functions of several complex variables*. Englewood Cliffs, NJ: Prentice-Hall.
- [14] Helman, M., Laurain, D., Reznik, D., Garcia, R. (2022). Poncelet triangles: a theory for locus ellipticity. *Beitr. Algebra Geom.* [doi:10.1007/s13366-021-00620-0](https://doi.org/10.1007/s13366-021-00620-0).
- [15] Kimberling, C. (1993). Triangle centers as functions. *Rocky Mountain J. Math.*, 23(4): 1269–1286.

- [16] Kimberling, C. (2019). Encyclopedia of triangle centers. faculty.evansville.edu/ck6/encyclopedia/ETC.html.
- [17] Lang, S. (2002). *Algebra*. Graduate Texts in Mathematics. Springer-Verlag, New York, 3rd ed.
- [18] Moore, R., Kearfott, R. B., Cloud, M. J. (2009). *Introduction to Interval Analysis*. Philadelphia: SIAM.
- [19] Odehnal, B. (2011). Poristic loci of triangle centers. *J. Geom. Graph.*, 15(1): 45–67.
- [20] Reznik, D. (2019). Triangular orbits in elliptic billiards: Loci of points X(1) to X(100). GitHub Pages. dan-reznik.github.io/billiard-loci/.
- [21] Reznik, D. (2020). Playlist for “Loci of Triangular Orbits in an Elliptic Billiard: Elliptic? Algebraic?”. bit.ly/2RE0igc.
- [22] Reznik, D., Garcia, R., Koiller, J. (2020). The ballet of triangle centers on the elliptic billiard. *J. Geom. and Graphics*, 24(1): 079–101.
- [23] Reznik, D., Garcia, R., Koiller, J. (2020). Can the elliptic billiard still surprise us? *Math Intelligencer*, 42: 6–17.
- [24] Reznik, D., Garcia, R., Koiller, J. (2021). Fifty new invariants of N -periodics in the elliptic billiard. *Arnold Math. J.*, 7(3): 341–355.
- [25] Romaskevich, O. (2014). On the incenters of triangular orbits on elliptic billiards. *Enseign. Math.*, 60(3-4): 247–255.
- [26] Rozikov, U. A. (2018). *An Introduction To Mathematical Billiards*. Singapore: World Scientific Publishing Company.
- [27] Schenck, H. (2003). *Computational Algebraic Geometry, London Mathematical Society Student Text*, vol. 58. Cambridge: Cambridge University Press.
- [28] Schwartz, R., Tabachnikov, S. (2016). Centers of mass of Poncelet polygons, 200 years after. *Math. Intelligencer*, 38(2): 29–34.
- [29] Snyder, J. M. (1992). Interval analysis for computer graphics. *Computer Graphics*, 26(2): 121–129.
- [30] Sturmfels, B. (1997). Introduction to resultants, in applications of computational algebraic geometry. In: *Proceedings of Symposia in Applied Mathematics*, vol. 53. Providence, RI: American Mathematical Society, pp. 25–40.
- [31] Tabachnikov, S. (2005). *Geometry and Billiards*, vol. 30 of *Student Mathematical Library*. Providence, RI: American Mathematical Society.
- [32] Tabachnikov, S. (2019). Projective configuration theorems: old wine into new wineskins. In: S. Dani, A. Papadopoulos, eds., *Geometry in History*. Basel: Springer Verlag, pp. 401–434.
- [33] Weisstein, E. W. (2003). *CRC concise encyclopedia of mathematics*. Chapman & Hall/CRC, Boca Raton, FL, 2nd ed.

RONALDO GARCIA, INST. DE MATEMÁTICA E ESTATÍSTICA, UNIV. FEDERAL DE GOIÁS, GOIÂNIA, GO, BRAZIL
Email address: ragarcia@ufg.br

JAIR KOILLER, DEPT. DE MATEMÁTICA, UNIV. FEDERAL DE JUIZ DE FORA, JUIZ DE FORA, MG, BRAZIL
Email address: jairkoiller@gmail.com

DAN REZNIK, DATA SCIENCE CONSULTING, RIO DE JANEIRO, RJ, BRAZIL
Email address: dan@dat-sci.com

